

DEEP LEARNING APPROACH FOR THE CLASSIFICATION AND DETECTION OF DENTAL AND CRANIOFACIAL CONDITIONS

*Asif Raza*¹, *Usman Amjad*², *Muhammad Ahmed Zaki*², *Hira Farman*³

¹Sir Syed University of Engineering and Technology, Karachi, Pakistan

²NED University of Engineering and Technology, Karachi, Pakistan

³Iqra University, Karachi, Pakistan

E-mail: asif.raza@ssuet.edu.pk, usmanamjad@neduet.edu.pk,

mzaki@neduet.edu.pk, hira.farman@iqra.edu.pk

Artificial Intelligence (AI) provides everyday functions along with higher applications in the domain of medicine, particularly medical imaging. Due to the advancement of technologies and imaging tools, AI-powered machine learning models will soon be used on a routine basis in medical diagnostics and treatment. The development involves Deep Learning (DL) algorithms and Convolutional Neural Networks (CNN) which will be trained using a dataset of disease-related images. AI gains increasing significance in our lives and medical research. In craniofacial imaging, CNNs have gained popularity and are employed in numerous scientific studies. This research introduces a DL model that utilizes a dataset containing five distinct categories: cavities, crown fractures, gum diseases, malalignment, and receding gums. These conditions have been classified and detected using the pre-trained Mobile-Net model. Notably, this model demonstrates a high training and validation accuracy reaching 99,9% and an incredibly low error rate of 0,001%.

Keywords: dental; mobile-net; deep learning; classification; detection.

Introduction

Artificial intelligence is increasingly important in our everyday lives and such domains as medical science, particularly medical imaging. Machine learning models are essential in medical treatment and diagnostics, particularly in dental, oral, and craniofacial imaging, where convolutional neural networks are gaining popularity. This manuscript explores the core principles of machine learning, outlines its advancements and recent applications in dental imaging, addresses existing challenges, and assesses the prospects for this scientific field [1].

Specifically, tooth marking on 3D dental surface models is an important aspect of orthodontic treatment planning. However, this sometimes proves challenging due to variations in the appearance of individual patients in terms of their pearly whites. Automatic tooth marking using intraoral scanners is ineffective because raw surfaces as taken by intraoral scanners tend to be inferior, especially within gingiva and deep intraoral recesses. Even though current end-to-end approaches, such as PointNet, demonstrate promising results, capturing the local, detailed geometric context needed to identify small teeth with variable shapes and appearances still remains a challenge. This paper introduces MeshSegNet, a deep-learning technique specifically designed to mark automatically raw dental surfaces. MeshSegNet utilizes numerous raw surface features to acquire multi-scale local contextual features through the use of graph-constrained learning modules and dense fusion of local and global geometric features for the precise annotation of mesh cells. Final segmentation follows after the graph-cut refinement in the predictions by MeshSegNet.

The analysis of a real-patient dataset with raw maxillary surfaces captured by 3D intraoral scanning clearly shows that MeshSegNet can outperform any other state-of-the-art deep learning method validated by cross-validation experiments performed on a 5-fold split [2].

The reconstruction of 3D dental models from Cone Beam Computed Tomography (CBCT) images has become necessary in orthodontics, implantology, and other dental diagnostics and treatment planning fields. Thus, a new method based on deep learning with U-net and attention gates was developed for the segmentation of tooth roots. Since the connections between the adjacency slices of a sequence of CBCT sequences are deemed to be high, it was proposed to use the Recurrent Neural Network and consider both intra-slice and inter-slice context. The network was evaluated based on 24 sets of images from CBCT sequences as training data and 361 images from 5 image sets as testing data. Segmentation accuracy metrics from testing on the dataset included 0,914 intersections over union, 0,955 DICE, 95,8% APR, 95,3% ARR, and an ASSD of 0,145 mm on average [3].

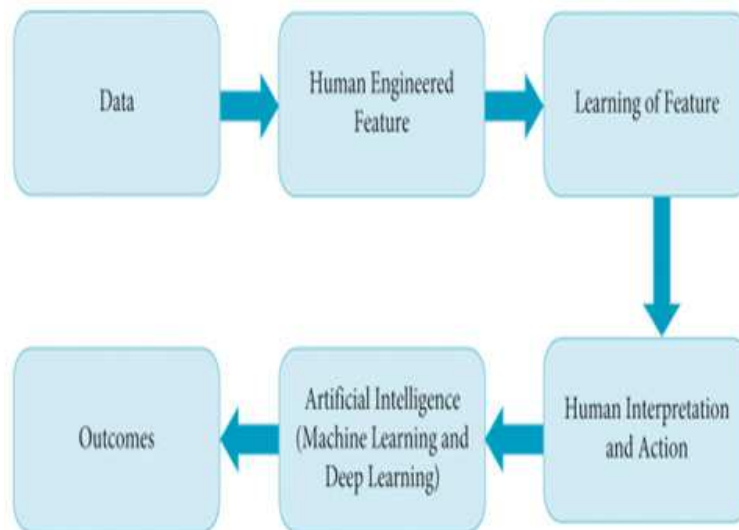


Fig. 1. Diagrammatic illustration of an Artificial Intelligence Model

Artificial intelligence (AI) systems, including deep CNNs, are advancing in medicine, especially in diagnostics and predictive analysis, as shown in the Fig. 3. A promising area for AI application is dental X-ray analysis, as these images often reveal issues that may be overlooked in routine checkups. However, such factors as poor image quality and human fatigue can lead to inconsistent and challenging diagnoses. This study introduces a new AI system which can automatically detect teeth and identify dental issues in panoramic X-rays, aiming to help healthcare professionals make more accurate and timely diagnoses. The system was developed using an extensive set of dental X-rays collected from various clinics. It can identify 14 distinct dental issues [4].

A rapid image processing-based detection method has been developed to streamline manual parameter measurement in clothing wires. This method uses an industrial camera for the real-time capturing of images of wires along the production line. First, the focus of interest within each image is identified based on unique characteristics. Image processing techniques such as filtering, motion de-blurring, and binarization are applied. The polar rotation technique with linear extrapolation is subsequently used to extract the edge of the wire, capturing the pixel coordinates of the tooth edge. Lastly, the curvature scale space

technology refines the extraction of feature points, enabling the precise measurement of parameters like tooth tip distance, tooth tip angle, and tooth tip edge length [5].

The advancement of artificial intelligence (AI) in dentistry lags behind other healthcare fields. Automation, such as segmentation and lesion detection in dental cone beam computed tomography (CBCT) images, is much needed. CBCT is a widely used dental imaging technique. However, research on deep learning-based automated segmentation is limited because of the complexity of the oral cavity, variations within each CBCT image, and the difficulty of obtaining a sufficient number of high-quality marked images for training [6]. Estimating the human chronological age is important in medical procedures. Teeth can be used for this purpose, and some techniques have been developed for age estimation based on tooth measurements in orthopantomogram (OPG) images. However, these methods are time-consuming, subjective for the observer, and have been tested only on high-quality OPG images. To address these issues, this work proposes two fully automatic methods for estimating the chronological age based on OPG images. The first method (DANet) uses a CNN to forecast age, while the following method (DASNet) adds another CNN to predict the presence of dental characteristics that could affect age estimation [7].

Fully convolutional neural networks (FCNs), such as U-Net, have been effective in segmenting medical images. We specifically applied U-Net to the challenging task of dental panoramic radiograph segmentation. To enhance segmentation accuracy, we employed the following techniques: Combining multiple networks (ensemble learning); Data modification during testing to improve performance; Leveraging data symmetry to upgrade segmentation; Incorporating lower-quality annotations to expand the training dataset. Our method was verified on a diverse dataset of 1500 dental panoramic radiographs. A single network used 1201 images for training to achieve a Dice score of 0,934. The merge of multiple networks (ensemble) allowed improving the score to 0,936 [8]. Section 1 of this paper provides a brief introduction; Section 2 reviews literature on machine learning related to dental radiography. Section 3 presents research methodology; Section 4 contains conclusions and covers future lines of research.

1. Literature Review

We used a dataset of 88 dental images captured with an intra-oral camera to frame a Deep Learning model (Mask R-CNN) that can identify and classify tooth decay on chewing surfaces. The model was used without any image preparation and leveraged superpixels for expert annotation and assessment. During training, the model used transfer learning and data augmentation techniques. The study details the technical aspects, presents preliminary findings, and highlights areas for improvement through fine-tuning the model and expanding the dataset [9].

As 3D sensors and networks connect the real world, more 3D applications appear. However, understanding these scenarios with fixed programs is challenging. Data-driven methods are needed to process 3D data, which drives up 3D Deep Learning demand. This experiment uses Point Net++, a feature extraction method, to generate an end-to-end deep learning system. It optimizes the network structure and parameters to enhance classification accuracy. The network is then applied to a dental model for classification and identification, which allows viewing the model from different perspectives [10].

This study focuses on dentistry, a medical field that deals with the tooth structure, growth, and diseases. Good oral hygiene is crucial for various essential activities, such as speaking, smiling, tasting, touching, digesting food, and swallowing. It is also essential for expressing emotions through facial movements. Human comfort in performing these activities is linked to self-esteem. Panoramic radiographs are a helpful tool for the simultaneous diagnostics of multiple oral diseases. However, the need for expert interpretation and the time it takes can be a burden. To address this issue, an automated approach has been developed to identify and classify disorders more efficiently. The study is based on a database of 500 images demonstrating six different types of oral diseases [11].

The early detection of dental plaque is crucial to prevent gum diseases and tooth decay. However, plaque is hard to see without special dyes because it is similar in colour to teeth. This paper presents a new low-shot learning technique that uses oral endoscope images to automatically segment dental plaque. The key innovation is to apply low-shot learning at the super-pixel level when the algorithm analyzes small, local areas of the image. The algorithm can better identify plaque by combining local (colour distribution) with global features (local-to-global structure) [12].

The application of machine learning to real-world scenarios involves two key components: data and features are the first one and models and algorithms are the second. Preprocessed and manually labelled data are introduced into a popular machine learning procedure for training and testing. A mature model is finalized after optimization and evaluation using a subset of chosen machine learning algorithms for data learning, as shown in Fig. 2. Medical image processing consists of four steps: pattern recognition, image analysis, image preprocessing, and image acquisition. Obtaining pictures is the first step. CBCT, MRI, and X-ray machines, among other medical imaging devices, provide most images used in medical image processing [13].

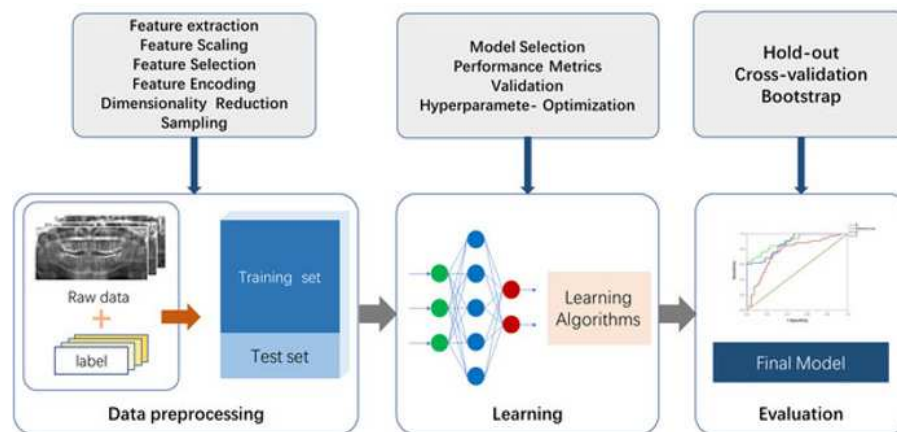


Fig. 2. Model Workflow

The authors present a new approach applying sparse voxels and 3D convolution neural networks (CNNs) to identify and categorize tooth types on 3D dental images. To overcome misclassifications in related tooth categories, we introduce a two-level hierarchical feature learning method. We also developed a three-level hierarchical segmentation method that utilizes deep convolution features for segmenting teeth from gums and adjacent teeth. To refine the boundaries of the gum lines and tooth gaps, we employ a conditional random field model [14].

A single pattern typically corresponds to a single kernel type. Applying filters to an image with a variety of kernel combinations allows extracting many distinct features from the picture. However, these pixel units will cause a strong response of the convolution outcome if there are kernels in a given image that correspond to the same patterns. Edges, directions, and other characteristics are among them. Furthermore, this process significantly reduces the number of weights because a filter performs convolution operations for each pixel unit of the CNN design image. It also suggests that different image units can share the parameters (parameter sharing function) [15]. The interpretability of the parameters will be enhanced by the successful extraction of spatial information from images processed by kernels. Convolution yields feature maps. Even after the image has been processed with filters, feature maps remain large. They can be further reduced by adding a pooling layer [16]. Although the pooling procedure and convolution operations are similar, they serve different purposes. Pooling filters are typically designed to yield the average or maximum value. Two methods – mean pooling and max pooling – are employed in the pooling layer to gather background data on feature points in the area and to extract texture information [17].

2. Methodology

2.1. Convolutional Neural Network

Machine learning has been transformed by the rise of ANNs inspired by biological neural networks. ANNs have become highly effective in machine learning tasks, often surpassing traditional AI techniques. CNNs stand out among ANN architectures because they can handle complex image recognition tasks. Their straightforward yet powerful design makes CNNs an ideal entry point for studying ANNs. This document provides a concise overview of CNNs, highlighting recent advancements and techniques in framing these robust image recognition models [18].

2.2. Batch Size

The first constant, `BATCH_SIZE`, is set to 128, indicating the number of data samples typically processed in each training batch. Batch size setting improves training efficiency by breaking the dataset into manageable chunks, conserving memory, and enabling parallel processing. The second constant, `IMG_SIZE`, is set as (299, 299), meaning that each image in the dataset will be resized to 299 pixels in width and 299 pixels in height. Consistent image dimensions are crucial for maintaining a uniform input across the dataset necessary for effective model training. 299x299 pixels are chosen because of the requirements for model architecture or the specific demands of the task at hand

2.3. Mobile-Net

The input shape and `IMG_SIZE` dimension are set to 3 for Mobile-Net. This parameter specifies the shape of the input data that the model will expect. Here, `IMG_SIZE` represents the desired dimensions for images, which is a tuple of (299, 299), indicating images resized to 299 pixels by 299 pixels. This parameter controls whether to include the fully connected layers at the top of the model. If we set it to `False`, the final fully connected layers responsible for classification are excluded. This is often done when the

model is used for transfer learning, where pre-trained convolutional layers are utilized, but classification layers are replaced or retrained for a specific task. Weights have been taken from the ImageNet. This parameter specifies weights to initialize the model. Setting it to ImageNet indicates that the model will be initialized with pre-trained weights obtained from training on the ImageNet dataset. These pre-trained weights provide a good initial point for numerous computer vision tasks and help improve the model performance, especially when the dataset for the target task is limited.

2.4. Training and Validation Accuracy

Each step took approximately 80 seconds in a training process lasting for 836 seconds. Training loss reached 7,8719 with an accuracy of 49,10%. During validation, the loss was 3,9547 with a validation accuracy of 73,08%. These metrics provide insights into the model performance and training progress. The training session spanned to 615 seconds; each step took approximately 56 seconds. Training loss reached 0,0085, indicating a high level of accuracy of 99,99%. During the validation phase, the loss increased slightly to 0,1050, though the validation accuracy remained high (97,20)%. These results suggest robust training performance and excellent generalization to unseen data, as shown in Fig. 3.

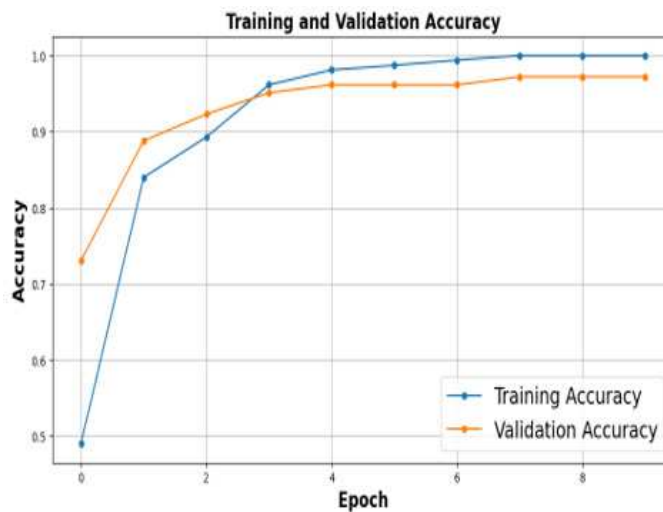


Fig. 3. Model Training and Validation Accuracy

2.5. Training and Validation Loss

The graph illustrates losses and epochs of the dataset of dental diseases and treatment by performing training and validation loss. Training loss starts with the epoch of 0,0 and the loss of 4,8 approximately. However, it has a downward trend and gives the values of both epochs and losses. Furthermore, it will be stopped by returning the epoch of at least 5,9 and the loss of 0. On the other hand, validation loss starts with the epoch of 0,0 and the loss of 3,2 approximately. However, it has a downward trend in the picture. After that, some variations will be taken; for example, when the loss is 0 and the epoch is 2,0 approximately, the value will run smoothly and constantly. Lastly, the values of both epochs will end at 16,4 at least and the value of loss will be 0 without any alteration. The graph gives some records of training and validation losses by collecting the facts and

figures to analyze the data through the use of the dataset of dental diseases, as shown in Fig. 4.

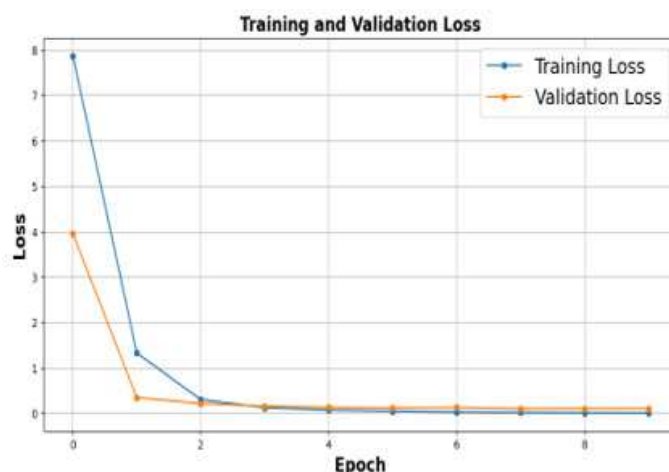


Fig. 4. Model Training and Validation Loss



Fig. 5. Model Training and Validation Error Rate

This graph shows error rates for both training and validation over ten training epochs in a machine-learning model. Initially, the training error rate decreases sharply, indicating that the model is learning well from the training data. The validation error rate also decreases though slightly slower, which suggests good generalization to unseen data. Both error rates stabilize toward the end, with the training error nearing zero, while the validation error remains slightly higher. This pattern implies that the model is well-fitted to the training data without overfitting significantly to it, as shown in Fig. 5.

2.6. Images Classes

The chart shows the relation between the number of images and the class of dental diseases: cavities, crown fractures, gum diseases, malalignment, and receding gums. Cavities start with 25 images in the given graph and then move upward by increasing the number of images from 25 to 310 approximately. Crown fractures start from 310 images. Their number further decreases to 225. Gum diseases start with 225 images and further decrease to 25 images. Malalignment starts with 25 images. After that, it will rise upward

and reach the value from 25 to 130 images. Lastly, receding gums start with 130 images, as shown in Fig. 6.

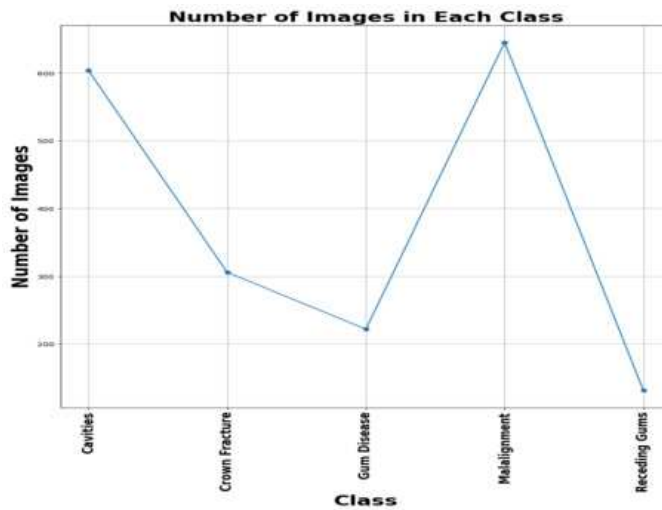


Fig. 6. Number of Images per class

There are five classes of images used to train the model. The classes have the following number of images: “Cavities” – 604 images, “Crown Fractures” – 306 images, “Gum Diseases” – 222 images, “Malalignment” – 645 images, and “Receding Gums” – 132 images. The training set totally contains 1,333 images. Testing and validation sets contain 288 images each.

Table 1

Confusion Matrix of Different Image Classes

Cavities	TP: 91	FP: 0	TN: 195	FN: 0
Crown Fracture	TP: 45	FP: 5	TN: 235	FN: 1
Gum Disease	TP: 28	FP: 1	TN: 253	FN: 4
Malalignment	TP: 96	FP: 1	TN: 188	FN: 1
Receding Gums	TP: 18	FP: 1	TN: 265	FN: 2

Where TP, FP, TN, and FN are True Positive, False Positive, True Negative, and False Negative values, respectively.

2.7. Confusion Matrix Validation and Training Process

The confusion matrix shown in the image evaluates the classification model performance on a validation dataset across five categories: Cavities, Crown Fractures, Gum Diseases, Malalignment, and Receding Gums. Each row represents actual labels, while each column represents predicted labels. Diagonal cells indicate correct predictions showing that 91 cases of Cavities, 45 case of Crown Fractures, 28 cases of Gum Diseases, 96 cases of Malalignment, and 18 cases of Receding Gums were correctly classified. Off-diagonal cells display misclassifications, where, for instance, one case of Crown Fracture was mistakenly classified as Gum Diseases, and one case of Receding Gums was misclassified as Malalignment. Colour intensity helps visualize these count; darker shades represent higher

counts, especially along the diagonal where most correct predictions are concentrated. The matrix shows that the model performs well and has few misclassifications, suggesting high accuracy in distinguishing among the categories, as shown in Fig. 7. This confusion matrix helps pinpoint specific areas where the model may need improvement, particularly in misclassified categories.

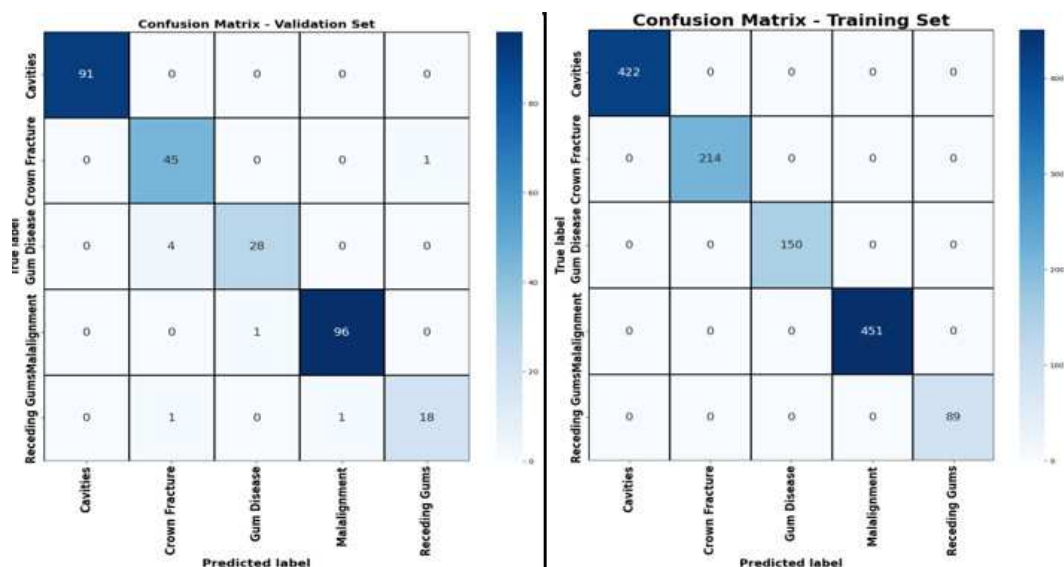


Fig. 7. Training and Validation Confusion Matrix

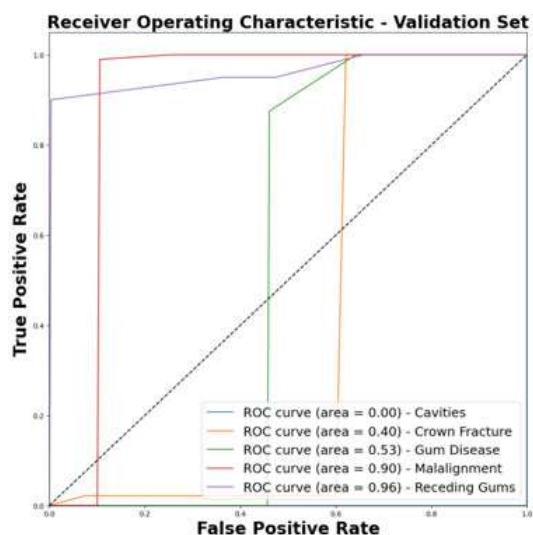


Fig. 8. Model ROC

This Receiver Operating Characteristic (ROC) curve evaluates the model performance on a validation set for detecting different dental conditions, as shown in Fig. 8. Each line represents the ROC curve for a specific condition, with the area under the curve (AUC) indicating performance. Higher AUC values indicate better diagnostic ability. Receding Gums and Malalignment have high AUC values (0,96 and 0,90, respectively), suggesting the model effectively distinguishes these conditions. In contrast, “Cavities” has an AUC of

0,00, indicating that performance is poor for that condition. Other conditions like Gum Diseases (AUC 0,53) and Crown Fractures (AUC 0.40) show moderate to low effectiveness. The closer each curve is to the upper left corner, the better the model performance for that condition.

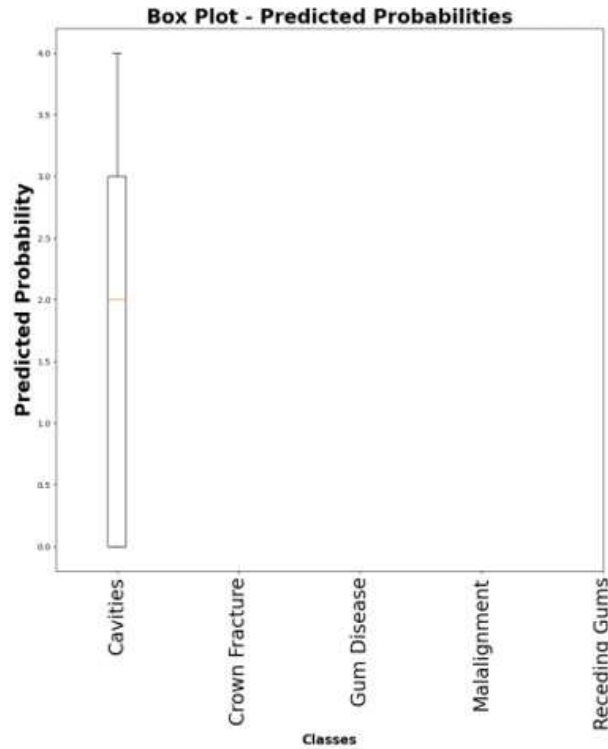


Fig. 9. Box Probabilities

2.8. Accuracy Metrics

Accuracy metrics for the classification model are as follows:

Table 2

Classification Report				
	Precision	Recall	F1-Score	Support
Cavities	1,00	1,00	1,00	91
Crown Fractures	0,90	0,98	0,94	46
Gum Diseases	0,97	0,88	0,92	32
Malalignment	0,99	0,99	0,99	97
Receding Gums	0,95	0,90	0,92	20
Accuracy	0,97	286		
Macro Avg,	0,65	0,95	0,95	286
Weighted Avg,	0,75	0,97	0,97	286

We received the following values: Cavities: Precision, Recall, and F1-score – 1,00 (for all the indicators), with support of 91 instances. Crown Fractures: Precision is 0,90, Recall

is 0,98, and F1-score is 0,94, with support of 46 instances. Gum Diseases: Precision is 0,97, Recall is 0,88, and F1-score is 0,92, with support of 32 instances. Malalignment: Precision, Recall, and F1-score are all 0,99, with support of 97 instances. Receding Gums: Precision is 0,95, Recall is 0,90, and F1-score is 0,92, with support of 20 instances. The overall accuracy of the model is 97% based on 286 instances. The macro average for Precision, Recall, and F1-score is 0,96, 0,95, and 0,95, respectively. The weighted average for Precision, Recall, and F1-score is 0,97, 0,97, and 0,97, respectively, considering the class imbalance.

Conclusion and Areas of Future Research

Artificial intelligence has become increasingly important in medical research, as well as our everyday lives. Its impact on medical imaging is particularly noticeable. Convolutional neural networks (CNNs) are popular in dental, oral, and craniofacial imaging and used increasingly in a growing number of scientific studies. The main contribution of our study is the introduction of a novel deep-learning model designed to take advantage of a privately selected dataset divided into five distinct categories. The key of this work is the strategic application of the pre-trained Mobile-Net model for the identification and categorization of complex oral, dental, and craniofacial disorders. This model is noteworthy for its exceptional performance metrics, including impressive training and validation accuracy. Deep learning can potentially transform the diagnostics and assessment of dental and craniofacial conditions, which holds great promise for the future of clinical practice and healthcare in general. Future research could benefit from the application of these modifications and optimizations, especially when it comes to investigating the integration of hybrid network architectures.

References

1. Ruiyang Ren, Haozhe Luo, Chongying Su, Yang Yao, Wen Liao. Machine Learning in Dental, Oral and Craniofacial Imaging: a Review of Recent Progress. *PeerJ Computer Science*, 2021, vol. 9, no. 29, 35 p. DOI: 10.7717/peerj.11451
2. Chunfeng Lian, Li Wang, Tai-Hsien Wu, Fan Wang, Pew-Thian Yap, Ching-Chang Ko, Dinggang Shen. Deep Multi-Scale Mesh Feature Learning for Automated Labeling of Raw Dental Surfaces From 3D Intraoral Scanners. *IEEE Transactions on Medical Imaging*, 2020, vol. 1, no. 1, pp. 2440–2450. DOI: 10.1109/tmi.2020.2971730
3. Qingqing Li, Ke Chen, Lin Han, Yan Zhuang, Jingtao Li, Jiangli Lin. Automatic Tooth Roots Segmentation of Cone Beam Computed Tomography Image Sequences using U-Net and RNN. *Journal of X-Ray Science and Technology*, 2020, vol. 28, no. 5, pp. 1–10. DOI: 10.3233/XST-200678
4. Muresan M.P., Barbura A.R., Nedevschi S. Teeth Detection and Dental Problem Classification in Panoramic X-Ray Images Using Deep Learning and Image Processing Techniques. *2020 IEEE 16th International Conference on Intelligent Computer Communication and Processing*, 2020, pp. 457–463. DOI: 10.1109/ICCP51029.2020.9266244
5. Min X., Haijin C. Research on Rapid Detection of Tooth Profile Parameters of the Clothing Wires Based on Image Processing. *2020 IEEE International Conference on Artificial Intelligence and Computer Applications*, 2020, pp. 586–590. DOI: 10.1109/ICAICA50127.2020.9182581
6. Zhiyang Zheng, Hao Yan, Frank C.S., Katherine J.S., Mel M., Jing Li. Anatomically Constrained Deep Learning for Automating Dental CBCT Segmentation and Lesion

- Detection. *IEEE Transactions on Automation Science and Engineering*, 2021, vol. 18, no. 2, pp. 603–614. DOI: 10.1109/TASE.2020.3025871
7. Vila-Blanco N., Carreira M.J., Varas-Quintana P., Balsa-Castro C., Tomas I. Deep Neural Networks for Chronological Age Estimation From OPG Images. *IEEE Trans Med Imaging*, 2020, vol. 39, no. 7, pp. 2374–2384. DOI: 10.1109/TMI.2020.2968765
 8. Koch T.L., Perslev M., Igel C., Brandt S.S. Accurate Segmentation of Dental Panoramic Radiographs with U-NETS. *2019 IEEE 16th International Symposium on Biomedical Imaging*, 2019, pp. 15–19. DOI: 10.1109/ISBI.2019.8759563
 9. Moutselos K., Berdouses E., Oulis C., Maglogiannis I. Recognizing Occlusal Caries in Dental Intraoral Images Using Deep Learning. *41st Annual International Conference of the IEEE Engineering in Medicine and Biology Society*, 2019, pp. 1617–1620. DOI: 10.1109/EMBC.2019.8856553
 10. Yiwen Liu, Xiuqin Shang, Zhen Shen, Bin Hu, Zhihai Wang, Gang Xiong. 3D Deep Learning for 3D Printing of Tooth Model. *IEEE International Conference on Service Operations and Logistics, and Informatics*, 2019, pp. 274–279. DOI: 10.1109/SOLI48380.2019.8955074
 11. Jaiswal P., Katkar V., Bhirud S. Multi Oral Disease Classification from Panoramic Radiograph using Transfer Learning and XGBoost. *International Journal of Advanced Computer Science and Applications*, 2022, vol. 13, no. 12. DOI: 10.14569/IJACSA.2022.0131230
 12. Shuai Li, Zhennan Pang, Song Wenfeng, Yuting Guo, You Wenzhe, Aimin Hao, Hong Qin. Low-Shot Learning of Automatic Dental Plaque Segmentation Based on Local-to-Global Feature Fusion. *IEEE 17th International Symposium on Biomedical Imaging*, 2020, pp. 664–668. DOI: 10.1109/ISBI45749.2020.9098741
 13. Incheol Kim, Misra D., Rodriguez L., Gill M., Liberton D.K., Almpani K., Lee J.S., Antani S. Malocclusion Classification on 3D Cone-Beam CT Craniofacial Images Using Multi-Channel Deep Learning Models. *2020 42nd Annual International Conference of the IEEE Engineering in Medicine and Biology Society*, 2020, pp. 1294–1298. DOI: 10.1109/EMBC44109.2020.9176672
 14. Tian Sukun, Dai Ning, Bei Zhang, Yuan Fulai, Yu Qing, Cheng Xiaosheng. Automatic Classification and Segmentation of Teeth on 3D Dental Model Using Hierarchical Deep Learning Networks. *IEEE Access*, 2019, vol. 7, pp. 84817–84828. DOI: 10.1109/ACCESS.2019.2924262
 15. Badrinarayanan V., Kendall A., Cipolla R. SegNet: A Deep Convolutional Encoder-Decoder Architecture for Image Segmentation. *IEEE Transactions on Pattern Analysis and Machine Intelligence*, 2017, vol. 39, no. 12, pp. 2481–2495.
 16. Milletari F., Navab N., Ahmadi S.-A. V-Net: Fully Convolutional Neural Networks for Volumetric Medical Image Segmentation. *Fourth International Conference on 3D Vision*, 2016, pp. 565–571. DOI: 10.1109/3DV.2016.79
 17. Jurdi R.El, Petitjean C., Honeine P., Abdallah F. BB-UNet: U-Net With Bounding Box Prior. *IEEE Journal of Selected Topics in Signal Processing*, 2020, vol. 14, no. 6, pp. 1189–1198. DOI: 10.1109/JSTSP.2020.3001502
 18. O’Shea K., Nash R. An Introduction to Convolutional Neural Networks. *arXiv: Neural and Evolutionary Computing*, 2015, 10 p. Available: <https://arxiv.org/abs/1511.08458>. DOI: 10.48550/arXiv.1511.08458

Received November 24, 2024

ПОДХОД ГЛУБОКОГО ОБУЧЕНИЯ ДЛЯ КЛАССИФИКАЦИИ И ОБНАРУЖЕНИЯ СТОМАТОЛОГИЧЕСКИХ И ЧЕРЕПНО-ЛИЦЕВЫХ ЗАБОЛЕВАНИЙ

Асиф Раза¹, Усман Амджад², Мухаммад Ахмед Заки², Хира Фарман³

¹Университет инженерии и технологий им. сэра Сайеда, г. Карачи, Пакистан

²Университет инженерии и технологий им. Надиршоу Эдулджи Диншоу, г. Карачи, Пакистан

³Университет Икра, г. Карачи, Пакистан

Искусственный интеллект (ИИ) обеспечивает повседневные функции наряду с более высокими приложениями в области медицины, в частности медицинской визуализации. Благодаря развитию технологий и инструментов визуализации модели машинного обучения на основе ИИ вскоре будут использоваться на постоянной основе в медицинской диагностике и лечении. Разработка включает алгоритмы глубокого обучения (DL) и сверточные нейронные сети (CNN), которые будут обучаться с использованием набора данных изображений, связанных с заболеваниями. ИИ приобретает все большее значение в нашей жизни и медицинских исследованиях. В черепно-лицевой визуализации CNN приобрели популярность и используются в многочисленных научных исследованиях. Это исследование представляет модель DL, которая использует набор данных, содержащий пять различных категорий: полости, переломы коронки, заболевания десен, неправильное расположение и рецессия десен. Эти состояния были классифицированы и обнаружены с помощью предварительно обученной модели Mobile-Net. Примечательно, что эта модель демонстрирует высокую точность обучения и проверки, достигающую 99,9% и невероятно низкий уровень ошибок 0,001%.

Ключевые слова: стоматология; мобильная сеть; глубокое обучение; классификация; обнаружение.

Асиф Раза, кафедра компьютерных наук и информационных технологий, Университет инженерии и технологий им. сэра Сайеда (г. Карачи, Пакистан), asif.raza@ssuet.edu.pk.

Усман Амджад, кафедра компьютерных наук и информационных технологий, Университет инженерии и технологий им. Надиршоу Эдулджи Диншоу (г. Карачи, Пакистан), usmanamjad@neduet.edu.pk.

Мухаммад Ахмед Заки, кафедра компьютерных наук и информационных технологий, Университет инженерии и технологий им. Надиршоу Эдулджи Диншоу (г. Карачи, Пакистан), mzaki@neduet.edu.pk.

Хира Фарман, кафедра компьютерных наук, Университет Икра (г. Карачи, Пакистан), hira.farman@iqra.edu.pk.

Поступила в редакцию 24 ноября 2024 г.